A Hybrid Nanoparticle System Integrating Tumor-derived Exosomes and Poly(amidoamine) Dendrimers: Implication for an effective gene delivery platform

Journal:	*Chemistry of Materials*
Manuscript ID	cm-2022-03705b.R2
Manuscript Type:	Article
Date Submitted by the Author:	n/a
Complete List of Authors:	Nair, Ashita; University of Wisconsin Madison, Pharmaceutical Sciences Javius-Jones, Kaila; University of Wisconsin - Madison, Pharmaceutical Sciences Division Bugno, Jason; University of Illinois at Chicago, Poellmann, Michael; University of Wisconsin-Madison, Pharmaceutical Sciences Division Mamidi, Narsimha; University of Wisconsin-Madison, Pharmaceutical Sciences Division (Wisconsin Center for NanoBioSystmes) Kim, In-San; Korea Institute of Science and Technology, Biomedical Research Institute Kwon, Ick Chan; Korea Institute of Science and Technology, Biomedical Research Center Hong, Heejoo; Asan Medical Center Hong, Seungpyo; University of Wisconsin Madison, Pharmaceutical Sciences

A Hybrid Nanoparticle System Integrating Tumor-derived Exosomes and Poly(amidoamine) Dendrimers: Implication for an effective gene delivery platform

*Ashita Nair[a]†, Kaila Javius-Jones[a]†, Jason Bugno[a,b], Michael J. Poellmann[a], Narsimha Mamidi[c], In-San Kim[d], Ick Chan Kwon[d], Heejoo Hong[e], and Seungpyo Hong[a, b, c, f, g]**

[a] Pharmaceutical Sciences Division, School of Pharmacy, University of Wisconsin, Madison, WI 53705, USA

[b] Department of Biopharmaceutical Sciences, College of Pharmacy, University of Illinois, Chicago, IL 60612, USA

[c] Wisconsin Center for NanoBioSystems, University of Wisconsin, Madison, WI 53705, USA

[d] Biomedical Research Center, Korea Institute of Science and Technology, Seoul, Republic of Korea 02792

[e] Department of Clinical Pharmacology & Therapeutics, Asan Medical Center, University of Ulsan, Seoul, Republic of Korea 05505

[f] Department of Pharmacy, Yonsei University, Incheon, Republic of Korea 21983

[g] Lachman Institue for Pharmaceutical Development, University of Wisconsin, Madison, WI 53705, USA

†Denotes the same contribution.

*Address all correspondence to:
Prof. Seungpyo Hong
Pharmaceutical Sciences Division, School of Pharmacy
University of Wisconsin-Madison
7121 Rennebohm Hall
777 Highland Avenue
Madison, WI 53705, USA
email: seungpyo.hong@wisc.edu
phone: (608) 890-0699

ABSTRACT

Nanoscale drug delivery systems for cancer treatment have demonstrated promising results in enhancing the selectivity of therapeutic agents while reducing their toxic side effects. However, several biological and physical barriers, such as the immunogenicity and undesirable biodistributions of such delivery systems, have hindered their fast translation. To address these issues, we have developed an exosome-dendrimer hybrid nanoparticle (NP) platform to combine the advantageous biological properties of natural exosomes and synthetic dendrimers into a single NP system. The novel hybrid NPs, consisting of exosomes derived from MCF7 cells and functionalized poly(amidoamine) (PAMAM) dendrimers, were prepared using sonication and characterized in terms of loading efficiency, size, cytotoxicity, and cellular interactions. Our results indicate that the loading of dendrimers into exosomes is dependent on dendrimer size and charge. The hybrid NPs inherited the size (~150 nm), surface charge (-10 mV), and surface protein markers (CD81, CD63) of exosomes. Importantly, the hybrid NPs enhanced cellular internalization of amine-terminated PAMAM dendrimers ($p < 0.05$), while exhibiting substantially lower cytotoxicity than the free positively charged dendrimers (113.3% vs. 35.6% of cell viability at 500 nM, $p < 0.05$). These advantageous properties of hybrid NPs were leveraged for use as a gene delivery vehicle, resulting in enhanced oligonucleotide delivery (over 2-fold) to cancer cells, compared to dendrimers alone. Furthermore, hybrid NPs effectively delivered small interfering RNA (siRNA) as well, downregulating programmed death-ligand 1 (PD-L1) expression significantly more (3.8-fold) than dendrimers alone ($p < 0.05$). Our results demonstrate that the individual characteristics of both exosomes and dendrimers can be integrated to generate a multifaceted NP platform, proposing a novel NP design strategy.

INTRODUCTION

Gene therapy allowing precise genetic manipulations, either for promotion or downregulation of target proteins, has long been considered a promising anticancer treatment option.[1–4] However, currently available anticancer gene therapeutic agents, such as plasmid DNA and RNA interference (RNAi), are afflicted with undesirable biodistribution properties, such as short half-life, degradation by nucleases, and inability to penetrate cells. These issues could be potentially addressed by employing a delivery vehicle that would allow the therapeutic agents to reach the target site in a viable form.[5,6] A myriad of nanoparticle (NP) delivery vehicles, including viral vectors, liposomes, and polymers, have been extensively studied to improve the stability and efficacy of these therapeutics. However, clinical translation of gene therapy has been disappointingly slow, primarily due to the fact that high gene therapy efficiency can be typically achieved at the cost of increased toxicity.

Poly(amidoamine) (PAMAM) dendrimers have been used to deliver genetic molecules for the treatment of various diseases.[7] These sub-10 nm hyperbranched hydrophilic polymers are characterized by well-defined nanoscale structures and pronounced surface group effects. The size and surface properties can be leveraged to enhance tumor penetration properties as well as support multivalent ligand binding at high density.[8–13] Similar to other cationic gene carriers, however, PAMAM dendrimers suffer from undesirable cytotoxicity and non-specificity due to electrostatic interactions with cell membranes.[14,15] Attempts to reduce cytotoxicity using partial acetylation and PEGylation strategies have resulted in diminished transfection efficiency.[16] Additionally, the small size of PAMAM dendrimers makes them subject to rapid renal elimination from circulation. To reduce the cytotoxicity, facilitate cell entry, and avoid the short

plasma circulation time of cationic PAMAM dendrimers, we have focused on designing novel gene delivery platforms through hybridization.

Our research group previously developed a hybrid NP design strategy to minimize the shortcomings of a single modality NP by combining two individual NPs such that the advantageous characteristics of both NPs are integrated into one system while negating their individual drawbacks.[17–20] One of the multi-scale hybrid NP systems was prepared by encapsulating PAMAM dendrimers into larger poly(ethylene glycol)-b-poly(lactide) (PEG-PLA) NPs.[19] Upon encapsulation, we showed that the hybrid NPs (approximately 100 nm in diameter) significantly improved biological behaviors of dendrimers, i.e., increased tumor accumulation via the enhanced permeability and retention (EPR) effect and prolonged plasma circulation.[20]

In parallel, similar approaches have been explored by others through hybridizing polymeric NPs with naturally occurring cell membranes such as platelets,[21] RBCs,[22] leukocytes,[23] MSCs,[24] and cancer cells.[25] Nanoscale extracellular vesicles, including exosomes, are also being explored as drug delivery systems.[26] Exosomes are secreted by cells and are known for their important role in communication among neighboring and distant cells.[27] Exosomes are implicated in several biological functions such as T-cell stimulation, antigen presentation, and tissue repair, by eliciting their responses through direct cell surface receptor binding or by transferring proteins and RNAs.[27–29] Being a natural messenger of information, the therapeutic potential of exosomes has been exploited both in their innate state (tissue regeneration,[30] immune modulation[31]) and as a delivery vehicle for small interfering RNA (siRNA),[32,33] microRNA (miRNA),[34] curcumin,[35] and doxorubicin.[36] Importantly, these naturally-occurring extracellular vesicles improved biocompatibility when compared to synthetic materials such as PAMAM dendrimers and PEG-PLA polymers.

In this paper, we have created a novel hybrid NP system to combine the advantageous biological properties of exosomes with the gene delivery potential of PAMAM dendrimers. By encapsulating dendrimers into exosomes, we anticipated the cellular interactions of hybrid NPs will primarily be driven by the exosomal lipid membrane and associated proteins, which would also efficiently mask the cytotoxic, electrostatic interactions of dendrimers with cells. We assessed the following three hypotheses in this study: i) positively charged dendrimers are efficiently hybridized with exosomes through electrostatic interactions; ii) exosomes reduce cytotoxicity of PAMAM dendrimers by masking the surface exposure of their primary amine groups; and iii) exosomes facilitate cell entry of dendrimers by multiple mechanisms of cellular uptake. In confirming these hypotheses, we demonstrate the potential for exosome-dendrimer hybrid NPs in gene delivery applications.

RESULTS

Characterization of Exosomes and Modified Dendrimers

Exosomes were isolated using a differential centrifugation method from cell culture media of either human mesenchymal stem cells (MSC) or a breast cancer cell line (MCF7). The isolated exosomes were characterized in terms of size, morphology, membrane potential, and protein markers using transmission electron microscopy (TEM), atomic force microscopy (AFM), nanoparticle tracking analysis (NTA), Zetasizer, and Western Blot analysis (**Figure S1**). Exosomes derived from MSC and MCF7 cell lines were respectively 139 nm and 156 nm in diameter while having the characteristic negative membrane zeta potential (-10.3 mV for MSC exosomes and -11.1 mV for MCF7 exosomes). Western blotting also revealed the presence of exosome protein markers, such as CD9, CD81, HSP70, and CD63, in both exosomes.[37] All these results confirmed that exosomes were successfully isolated from both MSC and MCF7 cultures.

PAMAM dendrimers of generation 2 (G2, 2.9 nm in theoretical diameter), G4 (4.5 nm), and G7 (8.1 nm) were labeled with rhodamine and modified to have either amine (positively charged, $-NH_2$), acetyl (neutrally charged, -Ac) or carboxyl (negatively charged, -COOH) surface groups using our previously published protocols.[11,38] The reaction scheme for the surface group modifications and the characteristic ^1H NMR spectra of modified dendrimers are shown in the supplementary material (**Scheme S1** and **Figures S2, S3,** and **S4**).

Loading Efficiency of Dendrimers into Exosomes

To systematically investigate the effect of dendrimer and exosome properties on hybrid NP formulation, we prepared a total of 18 configurations of hybrid NPs by varying the source of the

exosomes, along with dendrimer size and surface charge. Exosomes and dendrimers were hybridized via sonication (**Scheme 1**), a method commonly used to load drugs into exosomes without damaging the vesicle structure and surface proteins.[39–41] Throughout this paper, the term loading capacity was used to indicate the exosome properties, whereas loading efficiency was defined by the amount of dendrimers loaded into exosomes equivalent to 100 μg of exosomal proteins.

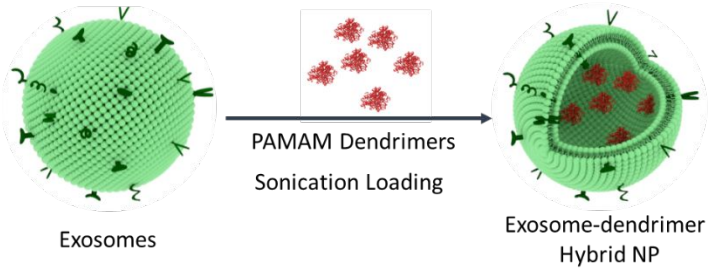

Scheme 1. Exosome hybridization with G2, G4, and G7 PAMAM dendrimers with either positively charged (NH_2), neutrally charged (Ac), or negatively charged (COOH) surface termini.

Loading efficiencies of the prepared dendrimers with various sizes and surface charges into exosomes are demonstrated in **Figure 1A.** Overall, both MCF7- and MSC-derived exosomes did not display any significant differences in terms of their loading capacity. However, significant differences in loading efficiency were observed depending on the size and surface charge of PAMAM dendrimers. The % loading of G7-NH_2, G7-Ac, and G7-COOH with MCF7 exosomes were measured to be 6.33 ± 1.99%, 0.69 ± 0.26%, and 0.20 ± 0.16%, respectively. This result clearly indicates that amine-terminated dendrimers could exhibit an order of magnitude greater loading into exosomes than acetylated or carboxylated dendrimers. Moreover, the quantity of cationic dendrimers hybridized with exosomes increased as dendrimer generation (size and terminal groups) increased from G2 to G7, given that the % loading of G2-NH_2, G4-

NH_2, and G7-NH_2 with MCF7 exosomes was found to be 0.51 ± 0.36%, 1.70 ± 0.16%, and 6.33 ± 1.99%, respectively. Such size-dependent increase, however, was not observed from either acetyl- or carboxyl-terminated dendrimers. These results demonstrate hybridization efficiency, or loading, is largely dependent on the physical properties of dendrimers, yet is independent of the source of exosomes. The hybrid NPs obtained from the positively charged G7-NH_2 and MCF7 exosomes exhibited the most efficient loading at approximately 6.3%.

The fact that the highest loading efficiency was observed from G7-NH_2 among the dendrimers tested indicates the hybridization process is likely dependent on electrostatic interactions between exosomes and dendrimers. To exclude any potential role played by exosomal proteins on the hybridization efficiency, we employed liposomes consisting of either net negative surface charge (anionic liposomes) or net positive surface charge (cationic liposomes), as a simplified model of exosomes. The lipid compositions and the measured zeta potential values of both liposomes are summarized in the supplementary material (**Table S1**). The loading efficiencies of various dendrimers into liposomes were then measured, as shown in **Figure 1B**. As expected, anionic liposomes with a zeta potential of -17.3 mV, which are similar to exosomes in terms of surface charge, showed the highest loading capacity with G7-NH_2 (3.73 ± 0.84 %). In contrast, the cationic liposomes (28.6 mV in zeta potential) exhibited the most efficient loading of G7-COOH (8.04 ± 1.33 %). These results confirm the primary driving force for hybridization between exosomes and dendrimers is charge-based interactions.

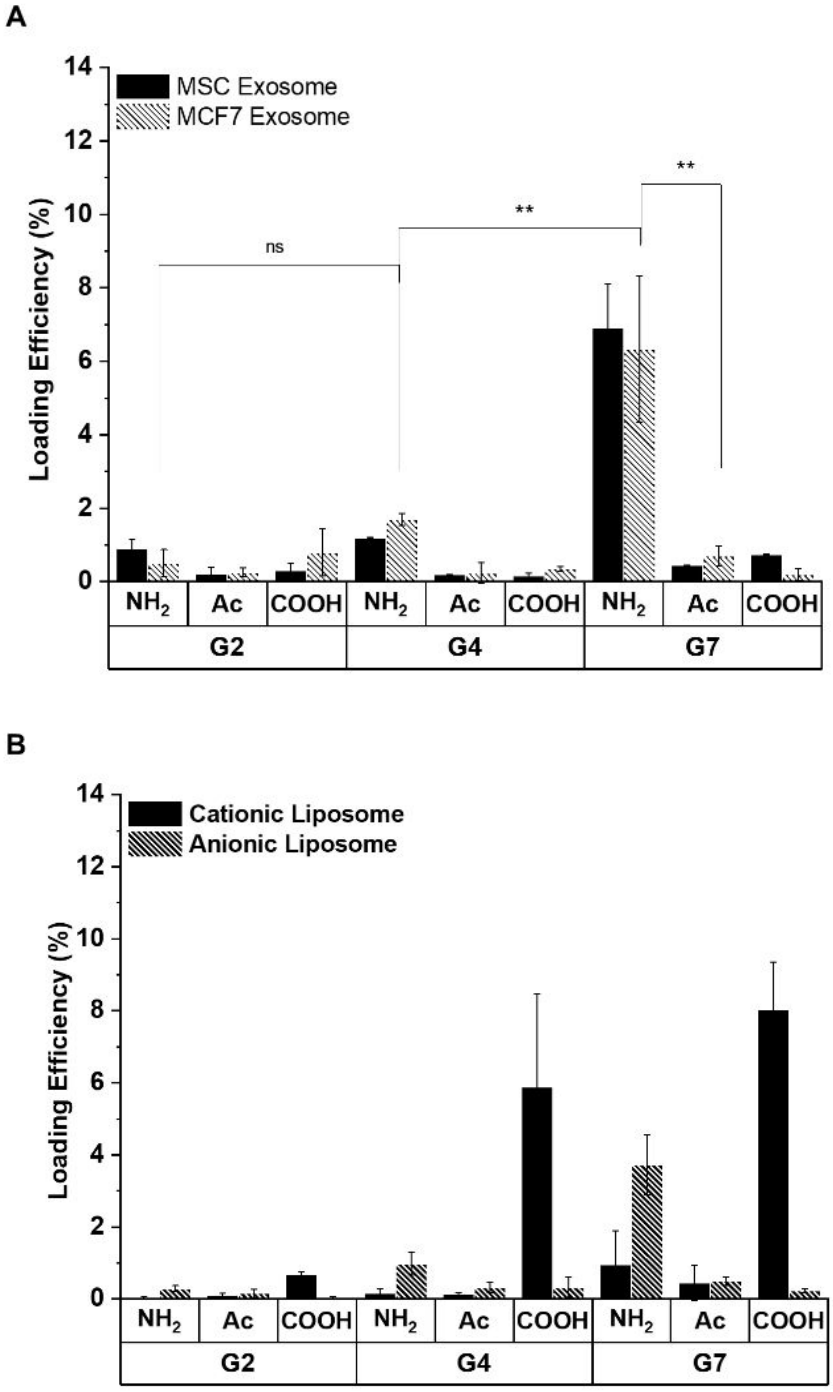

Figure 1. Loading efficiencies of various dendrimers into A) exosomes and B) liposomes. G7-NH_2 exhibits the maximum loading with the negatively charged exosomes at approximately 6.33 ± 1.99%, indicating that the loading efficiency is proportional to the size of dendrimers when

they are positively charged. Similar results obtained using cationic and anionic liposomes confirms the dependency of loading efficiency on electrostatic interaction.

Characterization of Hybrid NPs

Next, the hybrid NPs (MCF7/G4-NH_2, MCF7/G4-Ac, MCF7/G7-NH_2, and MCF7/G7-Ac) were characterized in terms of their morphology, size, and exosomal protein markers (**Figure 2**). The size and morphology of the hybrid NPs were measured and compared to each of the dendrimers and exosomes using AFM (**Figure 2A**). The hybrid NP system showed similar morphology to exosomes without any apparent aggregation. Whereas dendrimers and naïve exosomes presented uniform morphologies validating the original dendrimer size, and pure exosomes, respectively. These studies are supported by TEM and NTA analysis. Hybridization of MCF7 exosomes (~148 nm in diameter) with all dendrimers, including G4-NH_2 (8 nm), G4-Ac (8 nm), G7-NH_2 (20 nm), and G7-Ac (20 nm), did not result in a noticeable increase in size, generating hybrid NPs with approximately 150 nm in diameter, as measured using NTA (**Figure 2C).** The morphology of the hybrid NPs observed using TEM were consistent to that of free exosomes, and was not altered by dendrimer size and surface charge (**Figure 2B**). Furthermore, immunogold labeling of CD63 on hybrid NPs revealed vesicles formed with exosomal membranes in the correct orientation with membrane proteins on the external surface. Additionally, the western blot analysis for protein markers CD63 and CD81 confirmed hybrid NPs retained the membrane proteins of the exosome

after hybridization (**Figure 2D**). These results collectively indicate the hybrid NPs inherit the morphology, size, and membrane proteins of exosomes.

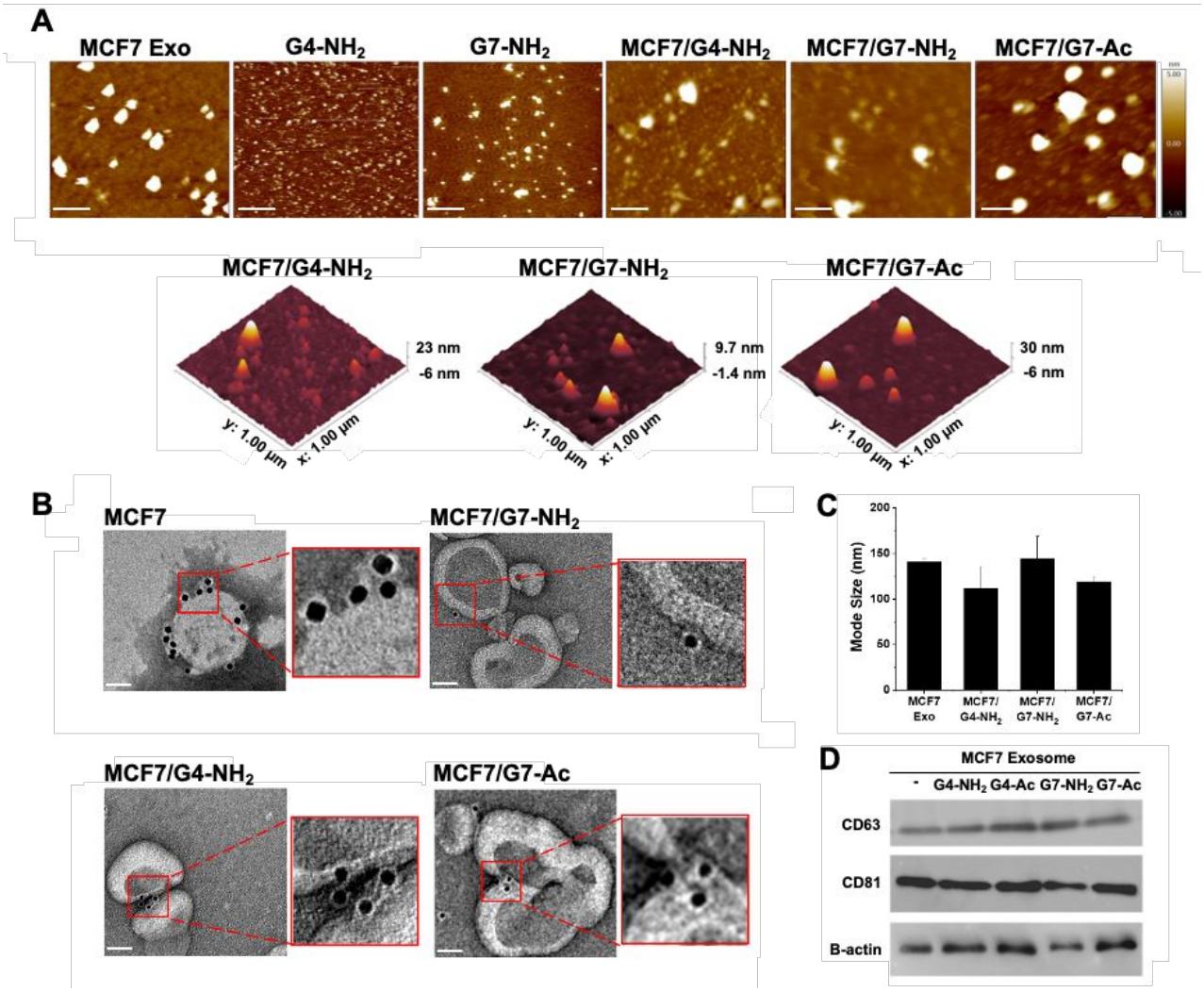

Figure 2. Physicochemical characterization of various nanoparticles used in this study. **A.** AFM images show that hybrid NP shape and diameters are similar to blank MCF7 exosomes, whereas the free dendrimers are signifcantly smaller. Scale bar: 200 nm. **B.** TEM confirms hybrid NP morphology and size. TEM immunogold staining to CD63 (gold nanoparticle-conjugated CD63 antibodies bound to CD63 proteins of exosomal membranes as shown in figure insets) also shows that the hybrid NPs retain the surface protein on the exosomal membranes. Scale bar: 50 nm. **C.** NTA analysis of the hybrid NPs provides additional confirmation of size. **D.** Western

blotting confirms the presence of exosome-enriched protein markers CD63 (26 kDa) and CD81 (25 kDa) in hybrid NPs.

Cytotoxicity of Hybrid NPs

Hybrid NPs inherit the membrane properties of the exosome including the surface charge (**Figure 3A, B**). The hybridization of MCF7 exosomes (-10 mV) with G4-NH_2 (7.54 mV) and G4-Ac (-1.85 mV) dendrimers generated hybrid NPs MCF7/G4-NH_2 and MCF7/G4-Ac, respectively, with -10 mV zeta potential. Similarly, hybridizing MCF7 exosomes with G7-NH_2 (57.3 mV) or G7-Ac (1.44 mV) generated MCF7/G7-NH_2 and MCF7/G7-Ac hybrid NPs, respectively, with -10 mV zeta potential. These results suggested the primary amines were masked in the hybrid NPs. We next examined the cytotoxicity of amine-terminated dendrimers by measuring the viability of MCF7 and MDA-MB-231 cells after 24 h treatment with G7-NH_2 and MCF7/G7-NH_2 (**Figure 3C, D**). Hybridization of G7-NH_2 with MCF7 exosomes markedly improved the cell viability of MCF7 ($79.6 \pm 14.1\%$ vs. $44.7 \pm 6.3\%$ at 500 nM, $p < 0.05$) and MDA-MB-231 cells ($113.3 \pm 17.28\%$ vs. $35.6 \pm 4.1\%$ at 500 nM, $p < 0.05$) compared to dendrimer alone. Branched poly(ethyleneimine) (bPEI), a cationic vector commonly used for gene delivery, was used as a positive control with cytotoxicity statistically equivalent to G7-NH_2. We concluded that hybridization effectively counters the cytotoxic characteristics of the amine-terminated dendrimers by masking the surface charges, supporting hypothesis ii.

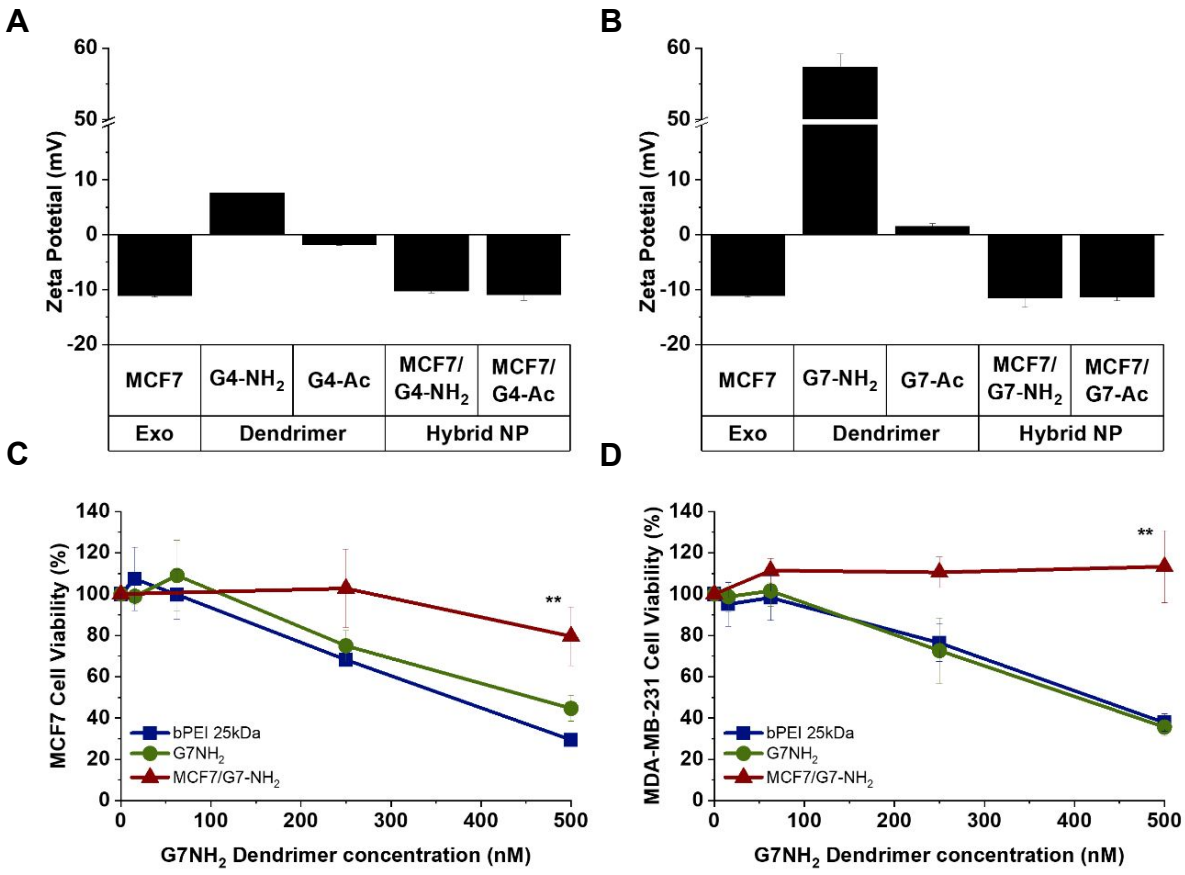

Figure 3. Hybrid NPs exhibit reduced cytotoxicity compared to G7-NH_2 **A.** The net charge of hybrid NPs containing G4-NH_2 or G4-Ac resembles the net charge of exosomes alone rather than either dendrimer. **B.** The net charge of hybrid NPs containing G7-NH_2 or G7-Ac was similarly equal to that of exosomes. **C.** Concentration dependence of MCF7 cytotoxicity. bPEI 25 KDa (■), G7-NH_2 (●), MCF7/G7-NH_2 (▲). **B.** Concentration dependence of MDA-MB-231 cells. Both conditions were quantified by CCK-8 assay after 24 h treatment. **$p < 0.05$.

Cellular Interaction of Hybrid NPs

We then investigated cellular interactions of PAMAM dendrimers, exosomes, and hybrid NPs upon incubation with two breast cancer cell lines, MCF7 (**Figure 4A** and **4B**) and MDA-MB-231, using confocal microscopy **(Figure 4C** and **4D**). Rhodamine-conjugated G7-NH_2 and

G7-Ac dendrimers were prepared, followed by hybrid NP formulations using MCF7 exosomes (MCF7/G7-NH_2 and MCF7/G7-Ac) . Based on our previous observations, G7-NH_2 dendrimers are readily taken up by cells.[11,38] The corresponding hybrid NPs resulted in significantly higher cellular uptake in both cell lines ($p < 0.05$). Interestingly, acetylated dendrimers, which exhibit minimal cellular interactions on their own, were also internalized when formulated as exosome-dendrimer hybrid NPs. Furthermore, differences in loading efficiency of G7-NH_2 (6.33%) and G7-Ac (0.69%) into hybrid NPs translated to the variances observed in cell uptake, as hybrid NPs with higher loading efficiency (MCF7/G7-NH_2) exhibited enhanced cell binding in a 6-hour incubation. The internalization of the dendrimers and hybrid NPs by MDA-MB-231 cells was also validated by acquiring z-stack images of the cells (**Figure S5B**). Moreover, the hybrid NPs appeared to remain intact for up to 48 h as seen by the colocalization of the dendrimer and exosome signals in the microscopy of MDA-MB-231 cells (**Figure S6**). Thus, we could conclude that the promoted cellular uptake of dendrimers was primarily due to the exosomal membranes.

In cancer pathology, exosomes have been implicated in the formation of the premetastatic niche, cancer progression, tumor growth, metastasis and drug resistance.[28,29,42] Exosomes in cancer not only communicate with neighboring cancer cells to transfer oncogenic signals and promote epithelial-mesenchymal transition (EMT) but also with the endothelial cells and immune cells in the stroma to promote pro-angiogenic, pro-metastatic and immune suppressive tumor microenvironment.[43] The role of exosomes in intracellular communication led us to determine if exosomes derived from cancer cells have specificity towards the parent cell line over other cancer cell lines. To test the specificity, hybrid NPs and empty exosomes were incubated with either MCF7 (parent cells, breast cancer cell line), MDA-MB-231 (metastatic

breast cancer cell line), or MiaPaCa2 (renal cancer cell line). Hybrid NPs were non-specifically taken up by all cell lines similar to naïve cancer exosomes (**Figure S7**). Consequently, exosome uptake was not specific to the parent cell line and was taken up by all cancer cells tested. Although hybrid NPs did not demonstrate specificity to parent cell lines, when compared to dendrimer-encapsulating liposomes, hybrid NPs exhibited enhanced cell uptake, indicating the enhanced cell binding by the exosomal membrane (**Figure S8**).

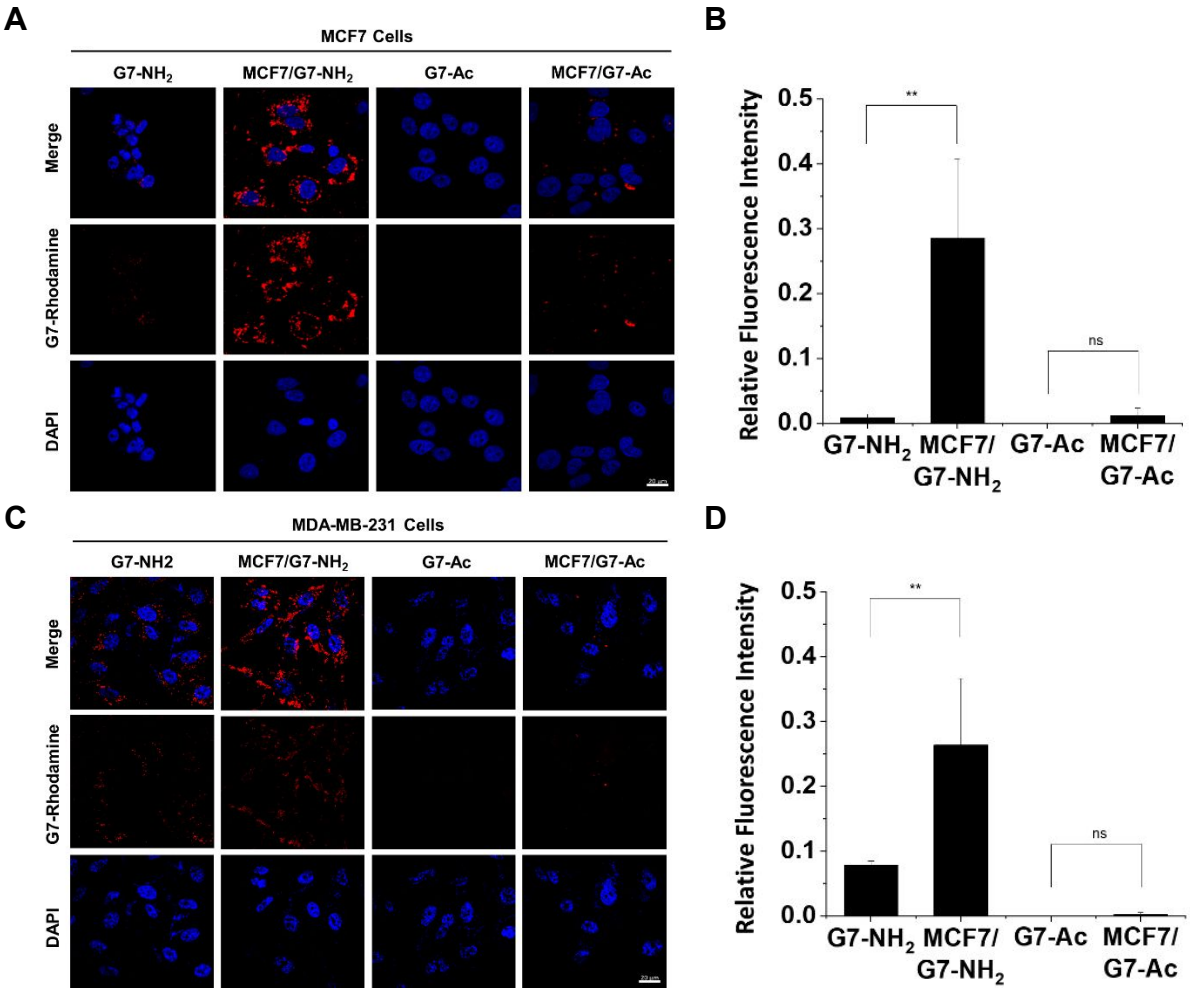

Figure 4. Cell uptake of dendrimers and hybrid NPs. The confocal laser scanning microscopy images of cell interaction of rhodamine-labeled dendrimers (G7-NH_2 and G7-Ac) and hybrid NP

(MCF7/G7-NH_2 and MCF7/G7-Ac) with MCF7 (**A**) and MDA-MB-231 (**C**) cells after 6 hours of treatment show greater cellular uptake in comparison to dendrimers alone. The cell uptake of the dendrimers by MCF7 (**B**) and MDA-MB-231 cells (**D**) was also quantified by their fluorescence intensity using ImageJ. Hybridization with exosomes enhances the cellular uptake of dendrimers in both cell lines. Scale bar: 20 μm, $^{**}p < 0.05$, ^{ns}p value not significant.

Cell Uptake Mechanism of Hybrid NPs

Exosomes enter the cell via multiple uptake mechanisms including protein receptor-mediated endocytosis,[44,45] membrane fusion,[46] clathrin-mediated endocytosis, macropinocytosis, and lipid-raft mediated endocytosis.[47] The uptake of cancer exosomes has also shown to be dependent on cell surface heparin sulfate proteoglycan (HSPG).[48] In contrast, cationic PAMAM dendrimers interact with cellular membranes primarily through electrostatic interaction and, to a smaller extent, through clathrin-mediated endocytosis.[49,50] The cell uptake mechanisms and their corresponding inhibitors are illustrated in **Figure 5A**. MDA-MB-231 cells were treated with uptake inhibitors prior to treatment with hybrid NPs for 4 hours followed by imaging with fluorescence microscopy (**Figure 5B**). Cellular uptake of G7-NH_2 was inhibited by quenching the surface amine charges with negatively charged polysaccharides heparin and chondroitin sulfate. It was also inhibited by clathrin protein inhibitor, chlorpromazine, and by inhibiting ATP by subjecting the cells to 4°C. The uptake of MCF7 exosomes was inhibited by heparin, an inhibitor of HSPG, or by proteinase K-mediated digesting of the surface proteins necessary for receptor-mediated endocytosis. Blocking the additional pathways of exosome uptake by cytochalasin D, MBCD, chlorpromazine, and treatment at 4˚C also led to decreased

internalization of exosomes. Consistent with our third hypothesis, the internalization of hybrid nanoparticles was reduced by the same inhibitors that blocked the uptake of naïve exosomes: heparin, 4°C, proteinase K, and Cytochalasin D **(Figure 5C)**. These results showed that the cellular uptake of hybrid NPs was driven by exosomal membrane interaction, rather than by electrostatic mechanisms that drive the uptake of cationic dendrimers.

A

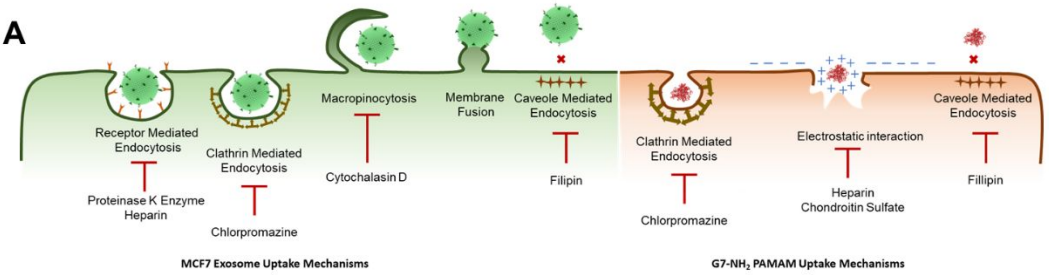

B

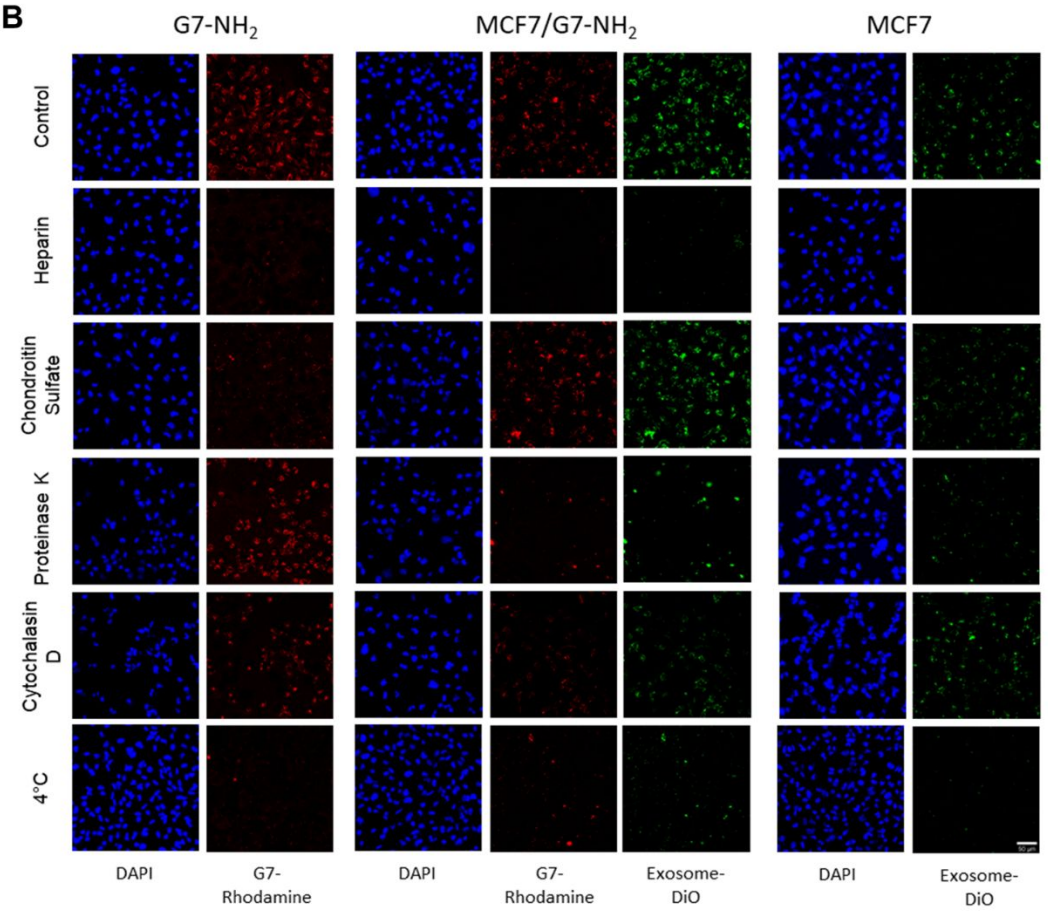

C

Cell Uptake Mechanism	Inhibitor	Inhibition of NP Cell Uptake		
		MCF7 Exosome	G7-NH2 PAMAM Dendrimers	MCF7/G7-NH2 Hybrid NPs
HSPG Mediated Uptake	Heparin	Yes	Yes	Yes
Electrostatic Interaction	Chondroitin Sulfate	No	Yes	No
Receptor mediated Uptake	Proteinase K Digestion	Yes	No	Yes
Macropinocytosis	Cytochalasin D	Yes	Yes	Yes
Energy Dependent Endocytosis	4°C	Yes	Yes	Yes

Figure 5. Cell uptake mechanisms of hybrid NPs. **A.** Illustration of various uptake mechanisms and corresponding inhibitors of exosomes and cationic dendrimers. **B.** Confocal laser scanning microscopy images of cell interaction of rhodamine-labeled dendrimers (G7-NH_2 and G7-Ac), DiO-labeled Hybrid NPs (MCF7/G7-NH_2 and MCF7/G7-Ac), and DiO-labeled MCF7 exosomes with MDA-MB-231 cells after 4 hours of treatment in presence of various cell uptake inhibitors. Scale bar: 50 μm **C.** Table summarizing the inhibitors affecting cell uptake of tested NPs. The cell uptake of the hybrid NPs is inhibited by heparin, proteinase K, cytochalasin D, and low-temperature treatment whereas chondroitin sulfate treatment did not affect the cell uptake process, similar to that of exosomes.

Gene Delivery Potential of Hybrid NPs

A Cy5-labeled oligonucleotide was used to explore the gene delivery potential of hybrid NPs. The labeled oligonucleotide was complexed with G7-NH_2 dendrimers at a nitrogen-to-phosphate ratio (N/P) of 20 before hybridizing with the exosomes, leading to a 65% loading efficiency. Hybrid NPs had a 5.3-fold increase in loading efficiency, as compared to exosomes alone (**Figure S9**). An N/P ratio of 10 led to a decreased loading efficiency of 30%, as the number of cationic groups post-gene complexation was reduced. We therefore fixed the N/P ratio at 20 for all subsequent experiments in this study. The hybridization of exosomes with G7-NH_2 also contributed to the improved loading of genetic material into exosomes. Compared to dendrimers and exosomes alone, hybrid NPs showed a 2-fold increase in oligonucleotide accumulation in cells as seen by the increased fluorescence intensity (**Figure 6**).

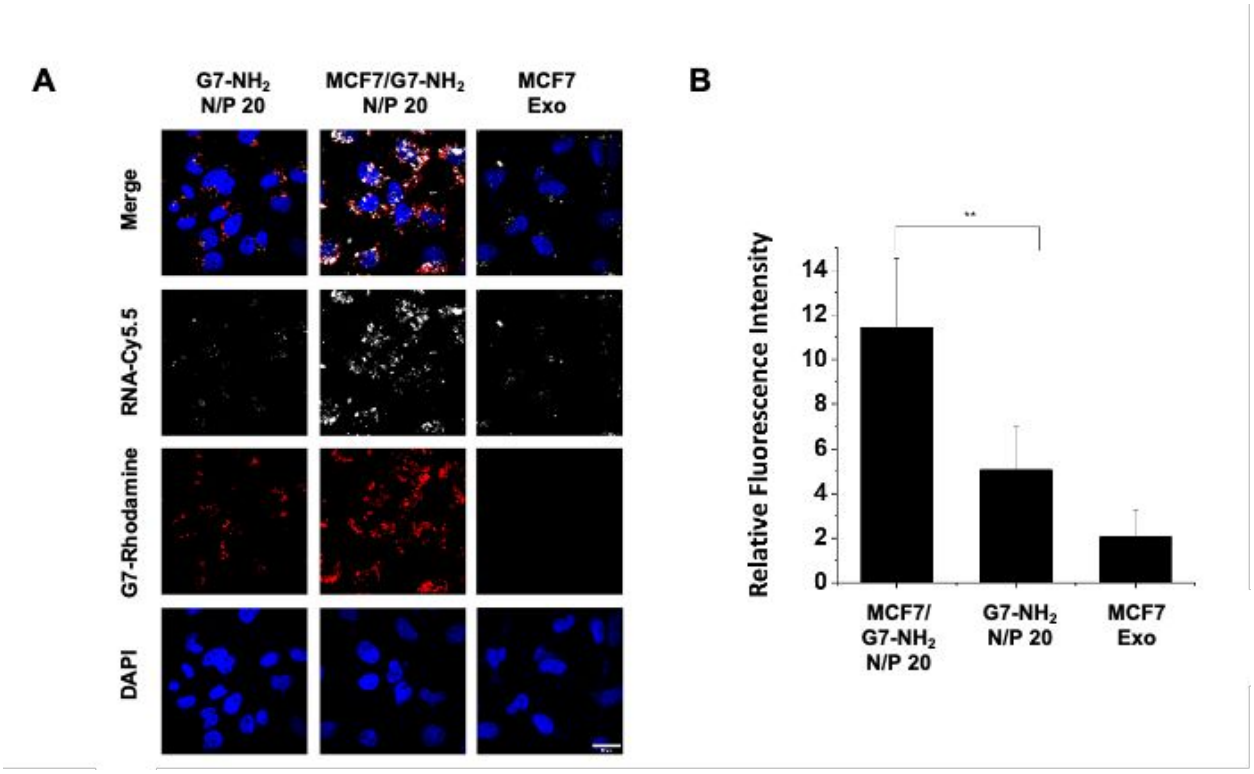

Figure 6. Enhanced gene delivery with hybrid NPs. **A.** Cy5-labeled oligonucleotide using G7-NH_2 PAMAM dendrimer, MCF7/G7-NH_2 hybrid NP at N/P ratio 20 or MCF7 exosomes as a gene delivery vehicle in MDA-MB-231 cells after 6 hours of treatment, visualized with laser scanning confocal microscopy. **B.** Quantified fluorescent signal suggested a 2-fold higher oligonucleotide delivery capacity by hybrid NPs compared to PAMAM dendrimers or exosomes alone. Scale bar: 20 μm, $^{**}p < 0.05$.

Next, we tested the transfection potential of the hybrid NPs with siRNA targeting programmed death-ligand 1 (PD-L1). PD-L1, an immune checkpoint inhibitor protein that interacts with programmed cell death protein 1 (PD-1) on immune cells, is frequently overexpressed by aggressive cancer cells and is associated with immune cell evasion for tumor leading to poor prognosis.[51] PD-L1 inhibitors, primarily monoclonal antibodies, block the detrimental PD-1/PD-L1 interaction and promote immune attack against cancer cells. As a gene therapy approach,

siRNA reduces the expression of PD-L1 in cancer cells, thereby decreasing the PD-L1-mediated immune evasion. Following interferon gamma (IFN-γ) treatment to induce the overexpression of PD-L1,[52] MDA-MB-231 cells were incubated with a 10 nM dose of PD-L1 siRNA delivered either with dendrimers, exosomes (N/P = 20), or hybrid nanoparticles. As shown in **Figure 7**, the delivery of PD-L1 siRNA with MCF7/G7-NH_2 NPs reduced the PD-L1 protein expression at the largest degree (by 59.2%) among the groups ($p < 0.05$), while G7-NH_2 dendrimer reduced expression by 15.6% only. The significant differences in transfection efficiency indicate that the hybrid NPs are less prone to the formation of protein corona that inhibits cellular update of gene-complexed NPs than free dendrimers.[53] As a result of the anionic exosomes offering limited interactions with serum proteins, exosomes alone also outcompeted dendrimers, exhibiting a 27.6% reduction in PD-L1 expression ($p < 0.05$).

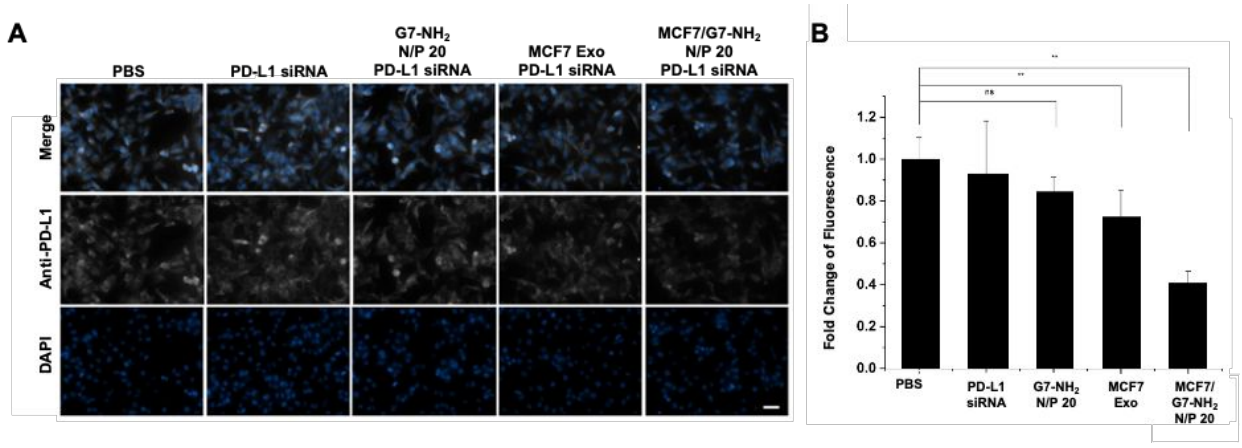

Figure 7: Hybrid NPs downregulate PD-L1 expression by delivering PD-L1 siRNA. **A.** PD-L1 siRNA (10 nM) was complexed with G7-NH_2 PAMAM dendrimer, MCF7 exosomes or MCF7/G7-NH_2 hybrid NP at N/P ratio 20 and incubated with MDA-MB-231 cells for 6 hours of treatment. **B.** Quantified fluorescent signal suggested a 3.8-fold reduction in PD-L1 protein

expression by hybrid NPs compared to dendrimers alone. Scale bar: 50 μm, $^{**}p < 0.05$, ^{ns}p value not significant.

DISCUSSION

In this study, we have demonstrated that cell entry and gene delivery by PAMAM dendrimers are greatly improved by hybridization with exosomes. We posed three hypotheses to assess the hybrid NPs concerning their cellular interaction and cytotoxicity. The first hypothesis addressed the mechanism of hybridization. Previous studies with cationic PAMAM dendrimers have demonstrated that their interactions with supported lipid bilayers and cell membranes are largely dependent upon the size and degree of the positive charge of the dendrimers.[15,54] Herein, we measured the hybridization efficiency of dendrimers with different surface charges and sizes with exosomes and liposomes comprised of well-defined lipid mixtures. Both exosomes and negatively charged liposomes hybridized most efficiently with dendrimers with positive surface charge. Larger-generation dendrimers with greater numbers of charged surface groups also hybridized more efficiently than smaller dendrimers with fewer surface charges. Thus, we concluded that the hybridization process was driven mainly by the electrostatic interaction between the terminal amines of the dendrimers and the negatively charged lipids of the bilayer, proving our hypothesis that the higher generation positively charged dendrimer would most efficiently hybridize with the exosomes.

The hybridization process did not adversely alter the exosomes' biological properties, such as membrane protein composition or vesicle morphology. The preservation of these features in the hybrid NP provides the biocompatibility and targetability that PAMAM

dendrimers lack. Our second hypothesis was that hybridization would mitigate cytotoxicity associated with the cationic PAMAM dendrimers. Despite their many advantages in drug and gene delivery, PAMAM dendrimers and similar cationic polymers cause membrane destabilization and cellular necrosis at high doses.[55] We theorized that hybrid NPs would effectively mask the primary amine groups on G7-NH_2, avoid detrimental interactions with the cell membrane, and ultimately reduce cytotoxicity compared to the dendrimers alone. The hybridization of dendrimers with exosomes indeed quenched the positive surface zeta potential and resulted in the characteristic negative zeta potential of the exosomes. Subsequent in vitro assays confirmed that cytotoxicity was effectively reduced in the hybrid NPs compared to dendrimers alone, indicating that our second hypothesis is valid.

The cellular interactions of PAMAM dendrimers are largely dependent upon their physical properties, such as size and surface charge.[15,20,38,56–58] In contrast, exosome interactions with cells are typically dictated by the composition of exosomal membrane proteins and lipids, which is highly dependent on the source of the vesicles.[59,60] The incorporation of exosome membrane proteins into the hybrid NPs and masking of the amine groups could also alter the cellular interaction of the PAMAM dendrimers. We thus posed our third hypothesis that hybridization would facilitate cellular uptake of PAMAM dendrimers by the same mechanisms as exosomes. Consistent with this hypothesis, we saw an increase in the uptake of the PAMAM dendrimers in the hybridized state and determined that the mechanisms were consistent with exosome uptake pathways. However, as the amine-terminated dendrimers exhibited a greater degree of cell entry than the acetylated dendrimers, the role played by dendrimer surface charge in affecting cell interactions of the hybrid NPs cannot be completed excluded. Instead, it seems

that both exosome surfaces and dendrimer charges collectively affect cell entry of the hybrid NPs through multiple mechanisms.

The ability of cationic dendrimers and exosomes as natural carriers of genetic materials has been utilized individually as a non-viral gene delivery system. In this work, we observed that hybrid NPs proved to be a better gene delivery vehicle than dendrimers alone. Non-viral gene delivery vehicles, such as polyethyleneimine (PEI) or PAMAM dendrimers, depend on their cationic nature to deliver genes to the cell. However, their cationic nature also leads to considerable cytotoxicity. Other approaches to decreasing dendrimer toxicity, such as partial acetylation of the cationic moieties, PEGylation, or modification with lipid chains, have been reported to decrease transfection efficiency.[61] It is therefore noteworthy that we observed higher delivery and transfection efficiency with hybrid NPs with reduced cytotoxicity. Hybrid NPs could ideally exploit the nucleotide complexation capacity of cationic dendrimers with the cell interaction and biodistribution properties of the exosome to deliver therapeutic genes to cancer cells. Additionally, exosome membrane proteins, such as CD47 with the ability to avoid clearance by monocytes, could potentially contribute to improved biodistribution *in vivo*.[62]

Future work will evaluate the biodistribution and biocompatibility properties of the hybrid NPs. We will also explore the potential of the exosome components to impart these biocompatibility properties to the hybrid system *in vivo*. Because the source of exosomes has a major influence on cellular interactions (as preliminarily shown in **Figure S10**),[59] we expect to also potentially modulate the biodistribution and uptake profile of hybrid NPs by collecting exosomes generated by different cell types.

CONCLUSION

We demonstrated the successful hybridization of exosomes derived from both MSC and MCF7 cells with PAMAM dendrimers to generate multifunctional hybrid NPs. This hybrid NP system offered the advantageous biological merits of exosomes as well as the gene delivery potential of PAMAM dendrimers within a single system. The hybrid MCF7/G7-NH_2 NP system exhibited the highest loading efficiency (~ 6.3%) and the experimental results reveal that charge-based interfaces are the key factors for the generation of a hybrid NPs system. We confirmed three hypotheses related to hybrid NP formations and their behaviors. First, we showed that hybridization was driven by the dendrimer charge. That is, positively charged, G7 PAMAM dendrimers showed the most efficient loading among the nine combinations evaluated. Second, we demonstrated that the hybrid NPs inherited the membrane properties of the exosomes, and as a result, evade the cytotoxicity associated with the positively charged PAMAM dendrimers. Specifically, the hybrid NP system exhibited improved cell viability against MCF7 and MDA-MB-231 cells likely owing to the masked surface charge of amine groups of the PAMAM dendrimer. Finally, we confirmed that the hybrid NPs enter cells via multiple mechanisms, primarily governed by the characteristics of exosomes. To explore the efficiency of the G7-NH_2-exosome hybrid NP system as a gene delivery vehicle, oligonucleotide uptake and siRNA delivery were also observed, resulting in a 2-fold increase in gene delivery potential and a 3.8-fold reduction in PD-L1 expression, compared to dendrimers alone, respectively. The

hybridization of PAMAM dendrimers with exosomes represents a promising approach to overcoming biological barriers to targeted therapeutics.

EXPERIMENTAL SECTION

Materials

Polyamidoamine (PAMAM) dendrimers with ethylenediamine core of generation 2, 4, and 7, bovine serum albumin (BSA), cholesterol, cytochalasin D, heparin, proteinase K, and human recombinant insulin were obtained from Millipore Sigma (St. Louis, MO). 5/6-carboxy-tetramethyl-rhodamine succinimidyl ester, mixed isomer (NHS-Rhodsmine), 3,3′-dioctadecyloxacarbocyanine perchlorate (DiO), and BCA Assay was purchased from Thermo Fisher Scientific Inc. (Waltham, MA). MCF7 and MiaPaCa2 cells were purchased from the American Type Tissue Collection (ATCC, Manassas, VA) and mesenchymal stem cells (MSC) were purchased from Lonza (Williamsport, PA). MEM Medium, MEM alpha media, DMEM media, penicillin/streptomycin antibiotics, and heat-inactivated fetal bovine serum (FBS) were purchased from Corning Incorporated (USA) (NY, NY). The MDA-MB 231 cells were a gift from Miyamoto lab at the University of Wisconsin-Madison. DOTAP (1,2-dioleoyl-3-trimethylammonium-propane (chloride salt)), DMPC (1,2-dimyristoyl-sn-glycero-3-phosphocholine), DOPE(1,2-dioleoyl-sn-glycero-3-phosphoethanolamine), and DOPS (1,2-dioleoyl-sn-glycero-3-phospho-L-serine (sodium salt)) were purchased from Avanti Polar Lipids Inc. (Alabaster, AL). Chondroitin Sulfate was purchased from Alfa Aesar (Tewksbury, MA).

Conjugation and Characterization of PAMAM Dendrimers

Dendrimers were conjugated to NHS-Rhodamine, and then surface modified, following the methods previously published.[38] Briefly, PAMAM dendrimers (G2-NH_2/9.2×10^{-6} mol, G4-NH_2/2.1×10^{-6} mol, G7-NH_2/0.26×10^{-6} mol) were dissolved in sodium bicarbonate buffer at pH 9.0. NHS- Rhodamine (18.4×10^{-6} mol for G2, 4.2×10^{-6} mol for G4, 2.1×10^{-6} mol for G7) was dissolved in DMSO was added dropwise to the dendrimer with constant stirring. The mixture was reacted for 24 hours at room temperature followed by membrane dialysis using a Spectra/Por dialysis membrane with MWCO 500 for G2, MWCO 3500 for G4, and MWCO 10,000 for G7 (Spectrum Laboratories Inc., Rancho Dominguez, CA) against water for purification. The purified dendrimers were freeze-dried using Labconco FreeZone 4.5 system (Kansas City, MO) and stored at −20 °C. The conjugation was confirmed using ^{1}H NMR using a Bruker Avance III HD 400 MHz NMR Spectrometer. Rhodamine-conjugated dendrimers were surface modified to have either a neutral charge by acetylation or a negative charge by carboxylation reactions. For the acetylation process, dendrimers in methanol (10 mg) were reacted with acetic anhydride (1.86×10^{-4} mol for G2, 2.10×10^{-4} mol for G4, 2.17×10^{-4} mol for G7) in presence of triethanolamine (1.25 molar excess of acetic anhydride) for 24 hours at room temperature. For the carboxylation process, the dendrimers in DMSO were reacted with succinic anhydride (1.86×10^{-4} mol for G2, 2.10×10^{-4} mol for G4, 2.17×10^{-4} mol for G7) for 24 hours at room temperature. The surface-modified dendrimers were purified by membrane dialysis, lyophilized and characterized by ^{1}H NMR as mentioned earlier.

Cell Culture

MCF7, MSC, MDA-MB-231, and MiaPaCa2 cells were cultured as a monolayer at 37°C, 5% CO_2 in complete media. For MCF7 cells, complete media was prepared using MEM Media supplemented with penicillin/streptomycin antibiotics (100 units/ mL), 10% heat-inactivated

fetal bovine serum (FBS), and 0.01 mg/ml human recombinant insulin. For MSC cells, complete media was prepared by supplementing MEM alpha media with penicillin/streptomycin antibiotics (100 units/ mL) and 10% heat-inactivated FBS. For MDA-MB-231 and MiaPaCa2 cells, the complete media consisted of DMEM Medium supplemented with penicillin/streptomycin antibiotics (100 units/ mL) and 10% heat-inactivated fetal bovine serum (FBS).

Exosome Isolation

Exosomes for all the experiments were isolated from the conditioned cell culture media of cultured MCF7 and MSC cells. To generate the conditioned media, the cells in monolayer were incubated in respective media supplemented with antibiotics and 1% bovine serum albumin for 48 hours. The exosome isolation process was carried out using the ultracentrifugation method as described by Thery *et al*.[37] Briefly, the collected media were centrifuged at 300 xg for 10 minutes to collect dead cells, followed by centrifugation at 12,000 xg for 30 minutes to collect any large cellular debris. The media were then centrifuged at 100,000 xg for 1 hour using a Beckman Type 45 Ti rotor and ultracentrifuge. The collected pellets were then washed with PBS and recentrifuged to remove any remaining media. The pelleted exosomes were resuspended in PBS and stored at -80°C till further use.

Preparation and Characterization of Hybrid NPs

For preparing the exosome-dendrimer hybrid NPs, a sonication process was used based on the exosome loading protocol described by Kim et. al.[40] Exosomes (50 µg as calculated by the amount of protein) were aliquoted in 500 µl of PBS and mixed with 10% w/w (to the exosome) dendrimer (5 µg). The mixture was sonicated using a QSonica Sonicator (20 kHz) with a 3.2 mm

probe at 20 % amplitude with 10-second on/off pulses for a total of 3 minutes followed by incubation at 37˚C for 30 minutes for the membranes to reform. To label the exosomes for microscopy, DiO Dye was added to the solution during the 37˚C incubation step. The free dendrimers and dye were isolated from the hybrids by ultracentrifugation at 100,000xg. The collected pellet, composed of hybrid NPs and exosomes, was resuspended in PBS and stored at -80°C till further use. The amount of dendrimers hybridized with the exosomes in the hybrid NPs were calculated using BCA assay and fluorescence intensity measurements with a Synergy microplate reader (Biotek). A series of dendrimer concentrations dissolved in a 1:1 solution of PBS: DMSO were used to generate a standard curve by measuring the fluorescence intensity of the rhodamine-conjugated to the dendrimer using the excitation and emission wavelengths of 540 nm and 580 nm respectively. Based on the fluorescence intensity of the samples dissolved in 1:1 PBS: DMSO, the standard curve was used to calculate the amount of dendrimers in the hybrid NPs. The amount of exosomes was measured as the amount of proteins estimated using BCA assay (Thermo Fisher) as per the manufacturer's protocol. The loading efficiency was calculated using the following formula: $Loading\ Efficicency\ (\%) = \frac{Amount\ of\ Dendrimer\ (\mu g)}{Amount\ of\ Exosomal\ Protein\ (\mu g)} \times 100$

Liposome preparation

Liposomes were prepared using the thin film hydration method followed by sonication as described previously.[63] The anionic liposome was generated by using DOPE:DMPC:Cholesterol:DOPS at a ratio 0.34:0.34:0.2:0.12[64] respectively whereas the cationic liposome was generated using DOTAP:DMPC:Cholesterol at a ratio 0.5:0.45:0.05 respectively. The respective lipid mixtures were dissolved in chloroform in a round bottom flask. The flask is connected to a rotary evaporator at RT for 30 minutes to completely evaporate the chloroform

and form a thin film. The dried film was hydrated with 1 ml PBS, followed by vortexing for 15 minutes and sonication with a tip sonicator for 1 minute to form either anionic or cationic liposome. Liposome-dendrimer hybrids were prepared using the protocol described in the hybridization process section.

Nanoparticle Tracking Analysis (NTA)

Diluted solutions of exosome and hybrid NPs were analyzed using the NS300 NTA instrument (Malvern Panalytical Ltd., Worcestershire, UK), with a 532 nm laser. 5 videos of 60 seconds each were collected for all samples and analyzed with Nanosight 3.0 software. The camera level was set at 14 and the detection threshold at 5 during the analysis.

Transmission Electron Microscopy (TEM)

The exosomes were characterized using TEM with negative staining as well as immunogold staining protocol. For the negative staining protocol, fixed exosome samples were adsorbed onto a 300 mesh Formvar/Carbon grid for at least 15 minutes. The grids were washed with water by floating on drops of water to remove PBS and contrasted with 1% uranyl acetate solution dye. These grids were used to validate the isolated exosomes. The immunogold staining procedure was carried out to test the presence of exosomal membrane proteins in hybrid NPs using antibodies against CD63. For immunogold staining, fixed hybrids NPs and exosomes were adsorbed onto a 300 mesh Formvar/Carbon grid and blocked with 0.1% BSA for 30 minutes. The grids were then washed and incubated overnight at 4°C with antibody against CD63 (polyclonal anti-CD 63 SC-15363, Santa Cruz). All the grids were rinsed and floated on 10 nm gold conjugated secondary antibody (EM Goat anti-Rabbit IgG: 10nm Gold, BBI Solutions) for 1 hour at room temperature. The grids were washed, fixed in 2% glutaraldehyde and contrasted

with 1% uranyl acetate solution. The grids were imaged with Tecnai T-12 TEM (FEI, Hillsboro, OR) and Gatan Ultrascan CCD camera (Gatan, Pleasanton, CA).

Atomic Force Microscopy (AFM)

AFM imaging was employed to assess the size of hybrid NPs. The dendrimers, exosomes and hybrid NPs were fixed with 2% glutaraldehyde and adsorbed onto a freshly cleaved mica for 30 minutes. The adsorbed samples in PBS were imaged using AC40 Biolever mini probe (Bruker AFM Probes) with nominal spring constant 0.09 N/m and tip radius 8 nm using an Asylum Infinity Biosystem (Oxford Instruments, Santa Barbara, Ca). A scanning area of 5 μm × 5 μm and 1 μm × 1 μm (256 x 256) was imaged at 1 kHz speed in tapping (AC) mode.

Western Blotting

The naïve exosomes and hybrid NPs were lysed using RIPA buffer and quantified for protein by BCA Assay. The proteins were resolved on an acrylamide gel and transferred onto a PVDF membrane in wet transfer conditions. The blot was blocked with 5% skim milk for 1 hour followed by overnight incubation in primary antibody against CD63 (polyclonal anti-CD63, SC-15363, Santa Cruz), CD81 (monoclonal anti-CD81 SC-166028, Santa Cruz), CD9 (monoclonal anti-CD81 SC-13118, Santa Cruz) and HSP70 (polyclonal anti-HSP70, EXOAB-Hsp70A-1, System Biosciences) at 4°C. Blots were incubated in secondary antibodies for 1 hour at room temperature and washed. The blots were developed using a chemiluminescent reagent, Clarity Western ECL Substrate (Bio-Rad) and imaged using Syngene G:Box F3 (Syngene, Frederick, MD).

Cell Uptake and Confocal Microscopy

MCF7, MDA-MB-231, and MiaPaca2 cells were seeded in 8-well chamber slides (Nunc™ Lab-Tek™ II Chamber Slide™ System, Thermo Scientific) at a density of 25,000 cells/well and incubated for 24 hours. Generation 7 amine dendrimers and generation 7 acetylated dendrimers and corresponding MCF7 exosome hybrid NPs were treated at 10 nM dendrimer concentration for 6 hours. Following treatment with the dendrimer, hybrid NPs, and exosomes, the cells were washed with PBS and then fixed in 4% paraformaldehyde for 10 min at room temperature. The fixed cells were washed and stained for the nuclei using a 1 μg/mL solution of Hoechst dye. The stained cells were washed and mounted using Prolong Gold mounting media and coverglass. The slides were imaged using Zeiss LSM 710 Confocal Microscope (CLSM, Carl Zeiss, Germany). The laser lines 405, 488, and 561 nm were used to excite Hoechst (nuclei), DiO (exosome membrane), and Rhodamine (dendrimer) respectively. The fluorescence intensity of rhodamine in each treatment was assessed from three independent runs using ImageJ software. The cell uptake mechanism of the hybrid NPs was carried out with MDA-MB-231 cells using G7-NH_2, MCF7 exosomes and MCF7/G7-NH_2 NPs. For receptor-mediated endocytosis inhibition, NPs were incubated with proteinase k enzyme at 100 μg/mL for 30 minutes at 37°C, followed by the addition of a protease inhibitor cocktail to inactivate the enzyme. For inhibition of charge-mediated cell interaction, the NPs were incubated with heparin or chondroitin sulfate at 10 μg/mL for 30 minutes before treating the cells. For inhibition of macropinocytosis and energy-dependent uptake process, the cells were treated with Cytochalasin D (5 μg/mL) or subjected to 4°C temperature for 30 minutes before treatment with the NPs for 4 hours.

Cytotoxicity Assays

MCF7 cells and MDA-MB-231 cells were seeded in a 96-well plate at a density of 12,000 cells/well and incubated for 24 hours. Cells were treated with branched polyethyleneimine 25

KDa, G7-NH_2, and MCF7/G7-NH_2 NPs at 6 concentrations (1000, 500, 250, 62.5, 15.25 nM) for 24 hours in serum-containing media. After the treatment period, the cell viability was assessed using Cell Counting Kit-8 Assay (CCK-8) (Enzo Life Sciences) as described by the manufacturer. Briefly, 10 µL of CCK-8 reagent was added to each well after NP treatment and incubated at 37˚C for 2 hours. The cell viability was determined by measuring absorbance at 450 nm using a plate reader. The cell viability was expressed normalized to the untreated cells.

Gene Transfection

MDA-MB-231 cells were seeded in 48 well plates. At 80% confluency, the cells were simulated with IFN-γ at 30 ng/mL for 6 hours to induce PD-L1 expression. The PD-L1 siRNA were complexed with dendrimers at a N/P ratio of 20, based on our previous studies[65-66]. The complexed dendrimers were treated as is or loaded into exosomes to form hybrid NPs. The hybrid NPs were formed as described in previous sections. The cells were treated with dendrimers, exosomes, or hybrid NPs complexed with PD-L1 siRNA for 6 hours in a complete medium. Post-treatment, media were changed, and cells were incubated for additional 48 hours. PD-L1 protein expression was checked using an immunofluorescence assay. Treated cells were washed with PBS, followed by blocking with 1% BSA solution. The cells were then incubated with primary antibody against PD-L1 (monoclonal anti-B7-H1 156-B7, R&D Systems) in a 1:200 dilution in 0.1% BSA at 4˚C for 4 hours. Next, cells were washed and incubated with 4 µg/mL of secondary antibody conjugated to AF647 (monoclonal anti-Rabbit IgG A-21244, Thermo Scientific) in 0.2% BSA at 4˚C overnight. Final step was to mount the cells and image with fluorescence microscopy.

Statistical Analysis

Statistical analysis was performed using OriginPro 8.1 (OriginLab, Northampton, MA). Mean cell viabilities were compared using 1-way ANNOVA followed by Tukey's post hoc test at $p < 0.05$.

ASSOCIATED CONTENT

Supporting Information. TEM and AFM images of isolated exosomes, western blot and ζ potential of exosomes, synthesis scheme and ^{1}H NMR spectra for modified dendrimers, microscopy images of ceullar interactions of various NP formulations, loading efficiency of oligonucleotide into exosomes. This material is available free of charge via the Internet at http://pubs.acs.org.

AUTHOR INFORMATION

Corresponding Author

*Address all correspondence to:

Prof. Seungpyo Hong

Pharmaceutical Sciences Division, School of Pharmacy

University of Wisconsin – Madison

7121 Rennebohm Hall

777 Highland Avenue

Madison, WI 53705, USA

email: seungpyo.hong@wisc.edu

phone: (608) 890-0699

Author Contributions

SH, HH, ISK, and ICK conceived the idea. SH provided experimental advice and funding support. SH, AN, KJJ, and JB designed the project. AN, KJJ, and MJP performed and interpreted the experiments. AN, KJJ, JB, MJP, NM, HH, and SH wrote the manuscript. All authors have approved the final version of the manuscript.

Funding Sources

This study was partially supported by National Science Foundation (NSF) under grants # DMR-1741560 and 1808251 and Milton J Henrichs Chair Fund.

ACKNOWLEDGMENT

The authors would like to thank Profs. J. Johnson, T. Bugni, G. Kwon, A. Bashirullah and M. Taylor in School of Pharmacy at the University of Wisconsin-Madison for their assistance with instrument usage. The authors would also like to thank J. Kim and E. Spreings for their assistance during the experimental setup.

REFERENCES:

(1) Pecot, C. V; Calin, G. A.; Coleman, R. L.; Lopez-Berestein, G.; Sood, A. K. RNA Interference in the Clinic: Challenges and Future Directions. *Nat. Rev. Cancer* **2011**, *11* (1), 59–67. https://doi.org/10.1038/nrc2966.

(2) Zuckerman, J. E.; Davis, M. E. Clinical Experiences with Systemically Administered SiRNA-Based Therapeutics in Cancer. *Nat. Rev. Drug Discov.* **2015**, *14* (12), 843–856. https://doi.org/10.1038/nrd4685.

(3) Greaney, S. K.; Algazi, A. P.; Tsai, K. K.; Takamura, K. T.; Chen, L.; Twitty, C. G.; Zhang, L.; Paciorek, A.; Pierce, R. H.; Le, M. H.; Daud, A. I.; Fong, L. Intratumoral Plasmid IL12 Electroporation Therapy in Patients with Advanced Melanoma Induces Systemic and Intratumoral T-Cell Responses. *Cancer Immunol. Res.* **2020**, *8* (2), 246–254. https://doi.org/10.1158/2326-6066.CIR-19-0359.

(4) Duperret, E. K.; Perales-Puchalt, A.; Stoltz, R.; Hiranjith, G. H.; Mandloi, N.; Barlow, J.; Chaudhuri, A.; Sardesai, N. Y.; Weiner, D. B. A Synthetic DNA, Multi-Neoantigen

Vaccine Drives Predominately MHC Class I CD8 þ T-Cell Responses, Impacting Tumor Challenge. *Cancer Immunol. Res.* **2019**, *7* (2), 174–182. https://doi.org/10.1158/2326-6066.CIR-18-0283.

(5) Xin, Y.; Huang, M.; Guo, W. W.; Huang, Q.; Zhang, L. zhen; Jiang, G. Nano-Based Delivery of RNAi in Cancer Therapy. *Mol. Cancer* **2017**, *16* (1), 134. https://doi.org/10.1186/s12943-017-0683-y.

(6) Pai, S. I.; Lin, Y.-Y.; Macaes, B.; Meneshian, A.; Hung, C.-F.; Wu, T.-C. Prospects of RNA Interference Therapy for Cancer. *Gene Ther.* **2006**, *13* (6), 464–477. https://doi.org/10.1038/sj.gt.3302694.

(7) Svenson, S.; Tomalia, D. A. Dendrimers in Biomedical Applications—Reflections on the Field. *Adv. Drug Deliv. Rev.* **2005**, *57* (15), 2106–2129. https://doi.org/https://doi.org/10.1016/j.addr.2005.09.018.

(8) Bugno, J.; Hsu, H.; Hong, S. Tweaking Dendrimers and Dendritic Nanoparticles for Controlled Nano-Bio Interactions: Potential Nanocarriers for Improved Cancer Targeting. *J. Drug Target.* **2015**, *23* (7–8), 642–650. https://doi.org/10.3109/1061186x.2015.1052077.

(9) Bugno, J.; Hsu, H.; Hong, S. Recent Advances in Targeted Drug Delivery Approaches Using Dendritic Polymers. *Biomater. Sci.* **2015**, *3* (7), 1025–1034. https://doi.org/10.1039/c4bm00351a.

(10) Hong, S.; Leroueil, P. R.; Majoros, I. J.; Orr, B. G.; Baker, J. R.; Banaszak Holl, M. M. The Binding Avidity of a Nanoparticle-Based Multivalent Targeted Drug Delivery Platform. *Chem. Biol.* **2007**, *14* (1), 107–115. https://doi.org/https://doi.org/10.1016/j.chembiol.2006.11.015.

(11) Bugno, J.; Hsu, H.-J.; Pearson, R. M.; Noh, H.; Hong, S. Size and Surface Charge of Engineered Poly(Amidoamine) Dendrimers Modulate Tumor Accumulation and Penetration: A Model Study Using Multicellular Tumor Spheroids. *Mol. Pharm.* **2016**, *13* (7), 2155–2163. https://doi.org/10.1021/acs.molpharmaceut.5b00946.

(12) Jeong, W. jin; Bu, J.; Han, Y.; Drelich, A. J.; Nair, A.; Král, P.; Hong, S. Nanoparticle Conjugation Stabilizes and Multimerizes β-Hairpin Peptides to Effectively Target PD-1/PD-L1 β-Sheet-Rich Interfaces. *J. Am. Chem. Soc.* **2020**, *142* (4), 1832–1837. https://doi.org/10.1021/jacs.9b10160.

(13) Bu, J.; Nair, A.; Iida, M.; Jeong, W. J.; Poellmann, M. J.; Mudd, K.; Kubiatowicz, L. J.; Liu, E. W.; Wheeler, D. L.; Hong, S. An Avidity-Based PD-L1 Antagonist Using Nanoparticle-Antibody Conjugates for Enhanced Immunotherapy. *Nano Lett.* **2020**, *20* (7), 4901–4909. https://doi.org/10.1021/acs.nanolett.0c00953.

(14) Halets, I.; Shcharbin, D.; Klajnert, B.; Bryszewska, M. Contribution of Hydrophobicity, DNA and Proteins to the Cytotoxicity of Cationic PAMAM Dendrimers. *Int. J. Pharm.* **2013**, *454* (1), 1–3. https://doi.org/https://doi.org/10.1016/j.ijpharm.2013.06.061.

(15) Hong, S.; Bielinska, A. U.; Mecke, A.; Keszler, B.; Beals, J. L.; Shi, X.; Balogh, L.; Orr, B. G.; Baker, J. R.; Banaszak Holl, M. M. Interaction of Poly(Amidoamine) Dendrimers with Supported Lipid Bilayers and Cells: Hole Formation and the Relation to Transport. *Bioconjug. Chem.* **2004**, *15* (4), 774–782. https://doi.org/10.1021/bc049962b.

(16) Fant, K.; Esbjörner, E. K.; Jenkins, A.; Grossel, M. C.; Lincoln, P.; Nordén, B. Effects of PEGylation and Acetylation of PAMAM Dendrimers on DNA Binding, Cytotoxicity and in Vitro Transfection Efficiency. *Mol. Pharm.* **2010**, *7* (5), 1734–1746. https://doi.org/10.1021/mp1001312.

(17) Sunoqrot, S.; Bae, J. W.; Jin, S.-E.; Pearson, R.; Liu, Y.; Hong, S. Kinetically Controlled Cellular Interactions of Polymer-Polymer and Polymer-Liposome Nanohybrid Systems. *Bioconjug. Chem.* **2011**, *22* (3), 466–474. https://doi.org/10.1021/bc100484t.

(18) Sunoqrot, S.; Bae, J. W.; Pearson, R. M.; Shyu, K.; Liu, Y.; Kim, D.; Hong, S. Temporal Control over Cellular Targeting through Hybridization of Folate-Targeted Dendrimers and PEG-PLA Nanoparticles. *Biomacromolecules* **2012**, *13* (4), 1223–1230. https://doi.org/10.1021/bm300316n.

(19) Sunoqrot, S.; Liu, Y.; Kim, D. H.; Hong, S. In Vitro Evaluation of Dendrimer-Polymer Hybrid Nanoparticles on Their Controlled Cellular Targeting Kinetics. *Mol. Pharm.* **2013**, *10* (6), 2157–2166. https://doi.org/10.1021/mp300560n.

(20) Sunoqrot, S.; Bugno, J.; Lantvit, D.; Burdette, J. E.; Hong, S. Prolonged Blood Circulation and Enhanced Tumor Accumulation of Folate-Targeted Dendrimer-Polymer Hybrid Nanoparticles. *J. Control. Release* **2014**, *191*, 115–122. https://doi.org/10.1016/j.jconrel.2014.05.006.

(21) Hu, C.-M. J.; Fang, R. H.; Wang, K.-C.; Luk, B. T.; Thamphiwatana, S.; Dehaini, D.; Nguyen, P.; Angsantikul, P.; Wen, C. H.; Kroll, A. V; Carpenter, C.; Ramesh, M.; Qu, V.; Patel, S. H.; Zhu, J.; Shi, W.; Hofman, F. M.; Chen, T. C.; Gao, W.; Zhang, K.; Chien, S.; Zhang, L. Nanoparticle Biointerfacing by Platelet Membrane Cloaking. *Nature* **2015**, *526*, 118. https://doi.org/10.1038/nature15373.

(22) Gao, W.; Hu, C. M.; Fang, R. H.; Luk, B. T.; Su, J.; Zhang, L. Surface Functionalization of Gold Nanoparticles with Red Blood Cell Membranes. *Adv Mater* **2013**, *25* (26), 3549–3553. https://doi.org/10.1002/adma.201300638.

(23) Parodi, A.; Quattrocchi, N.; van de Ven, A. L.; Chiappini, C.; Evangelopoulos, M.; Martinez, J. O.; Brown, B. S.; Khaled, S. Z.; Yazdi, I. K.; Enzo, M. V; Isenhart, L.; Ferrari, M.; Tasciotti, E. Synthetic Nanoparticles Functionalized with Biomimetic Leukocyte Membranes Possess Cell-like Functions. *Nat Nanotechnol* **2013**, *8* (1), 61–68. https://doi.org/10.1038/nnano.2012.212.

(24) Toledano Furman, N. E.; Lupu-Haber, Y.; Bronshtein, T.; Kaneti, L.; Letko, N.; Weinstein, E.; Baruch, L.; Machluf, M. Reconstructed Stem Cell Nanoghosts: A Natural Tumor Targeting Platform. *Nano Lett.* **2013**, *13* (7), 3248–3255. https://doi.org/10.1021/nl401376w.

(25) Sun, H.; Su, J.; Meng, Q.; Yin, Q.; Chen, L.; Gu, W.; Zhang, P.; Zhang, Z.; Yu, H.; Wang, S.; Li, Y. Cancer-Cell-Biomimetic Nanoparticles for Targeted Therapy of Homotypic Tumors. *Adv. Mater.* **2016**, *28* (43), 9581–9588. https://doi.org/10.1002/adma.201602173.

(26) El Andaloussi, S.; Mäger, I.; Breakefield, X. O.; Wood, M. J. A. Extracellular Vesicles: Biology and Emerging Therapeutic Opportunities. *Nat. Rev. Drug Discov.* **2013**, *12*, 347. https://doi.org/10.1038/nrd3978.

(27) Kowal, J.; Tkach, M.; Thery, C. Biogenesis and Secretion of Exosomes. *Curr Opin Cell Biol* **2014**, *29*, 116–125. https://doi.org/10.1016/j.ceb.2014.05.004.

(28) Zhang, Y.; Wang, X.-F. A Niche Role for Cancer Exosomes in Metastasis. *Nat. Cell Biol.* **2015**, *17*, 709. https://doi.org/10.1038/ncb3181.

(29) Ruivo, C. F.; Adem, B.; Silva, M.; Melo, S. A. The Biology of Cancer Exosomes: Insights and New Perspectives. *Cancer Res.* **2017**, *77* (23), 6480.

(30) Yeo, R. W.; Lai, R. C.; Zhang, B.; Tan, S. S.; Yin, Y.; Teh, B. J.; Lim, S. K. Mesenchymal Stem Cell: An Efficient Mass Producer of Exosomes for Drug Delivery. *Adv Drug Deliv Rev* **2013**, *65* (3), 336–341. https://doi.org/10.1016/j.addr.2012.07.001.

(31) Chaput, N.; Thery, C. Exosomes: Immune Properties and Potential Clinical Implementations. *Semin Immunopathol* **2011**, *33* (5), 419–440. https://doi.org/10.1007/s00281-010-0233-9.

(32) El Andaloussi, S.; Lakhal, S.; Mäger, I.; Wood, M. J. A. Exosomes for Targeted SiRNA Delivery across Biological Barriers. *Adv. Drug Deliv. Rev.* **2013**, *65* (3), 391–397. https://doi.org/https://doi.org/10.1016/j.addr.2012.08.008.

(33) Alvarez-Erviti, L.; Seow, Y.; Yin, H.; Betts, C.; Lakhal, S.; Wood, M. J. A. Delivery of SiRNA to the Mouse Brain by Systemic Injection of Targeted Exosomes. *Nat. Biotechnol.* **2011**, *29* (4), 341–345. https://doi.org/10.1038/nbt.1807.

(34) Momen-Heravi, F.; Bala, S.; Bukong, T.; Szabo, G. Exosome-Mediated Delivery of Functionally Active MiRNA-155 Inhibitor to Macrophages. *Nanomedicine Nanotechnology, Biol. Med.* **2014**, *10* (7), 1517–1527. https://doi.org/https://doi.org/10.1016/j.nano.2014.03.014.

(35) Sun, D.; Zhuang, X.; Xiang, X.; Liu, Y.; Zhang, S.; Liu, C.; Barnes, S.; Grizzle, W.; Miller, D.; Zhang, H.-G. A Novel Nanoparticle Drug Delivery System: The Anti-Inflammatory Activity of Curcumin Is Enhanced When Encapsulated in Exosomes. *Mol. Ther.* **2010**, *18* (9), 1606–1614. https://doi.org/https://doi.org/10.1038/mt.2010.105.

(36) Tian, Y.; Li, S.; Song, J.; Ji, T.; Zhu, M.; Anderson, G. J.; Wei, J.; Nie, G. A Doxorubicin Delivery Platform Using Engineered Natural Membrane Vesicle Exosomes for Targeted Tumor Therapy. *Biomaterials* **2014**, *35* (7), 2383–2390. https://doi.org/https://doi.org/10.1016/j.biomaterials.2013.11.083.

(37) Thery, C.; Amigorena, S.; Raposo, G.; Clayton, A. Isolation and Characterization of Exosomes from Cell Culture Supernatants and Biological Fluids. *Curr Protoc Cell Biol* **2006**, *Chapter 3*, Unit 3.22. https://doi.org/10.1002/0471143030.cb0322s30.

(38) Yang, Y.; Sunoqrot, S.; Stowell, C.; Ji, J.; Lee, C. W.; Kim, J. W.; Khan, S. A.; Hong, S. Effect of Size, Surface Charge, and Hydrophobicity of Poly(Amidoamine) Dendrimers on Their Skin Penetration. *Biomacromolecules* **2012**, *13* (7), 2154–2162. https://doi.org/10.1021/bm300545b.

(39) Haney, M. J.; Klyachko, N. L.; Zhao, Y.; Gupta, R.; Plotnikova, E. G.; He, Z.; Patel, T.; Piroyan, A.; Sokolsky, M.; Kabanov, A. V; Batrakova, E. V. Exosomes as Drug Delivery Vehicles for Parkinson's Disease Therapy. *J. Control. Release* **2015**, *207* (Supplement C), 18–30. https://doi.org/https://doi.org/10.1016/j.jconrel.2015.03.033.

(40) Kim, M. S.; Haney, M. J.; Zhao, Y.; Mahajan, V.; Deygen, I.; Klyachko, N. L.; Inskoe, E.; Piroyan, A.; Sokolsky, M.; Okolie, O.; Hingtgen, S. D.; Kabanov, A. V; Batrakova, E. V. Development of Exosome-Encapsulated Paclitaxel to Overcome MDR in Cancer Cells. *Nanomedicine Nanotechnology, Biol. Med.* **2016**, *12* (3), 655–664. https://doi.org/https://doi.org/10.1016/j.nano.2015.10.012.

(41) Kim, M. S.; Haney, M. J.; Zhao, Y.; Yuan, D.; Deygen, I.; Klyachko, N. L.; Kabanov, A. V; Batrakova, E. V. Engineering Macrophage-Derived Exosomes for Targeted Paclitaxel Delivery to Pulmonary Metastases: In Vitro and in Vivo Evaluations. *Nanomedicine Nanotechnology, Biol. Med.* **2018**, *14* (1), 195–204. https://doi.org/https://doi.org/10.1016/j.nano.2017.09.011.

(42) Kalluri, R. The Biology and Function of Exosomes in Cancer. *J Clin Invest* **2016**, *126* (4), 1208–1215. https://doi.org/10.1172/jci81135.

(43) Bebelman, M. P.; Smit, M. J.; Pegtel, D. M.; Baglio, S. R. Biogenesis and Function of Extracellular Vesicles in Cancer. *Pharmacol. Ther.* **2018**, *188*, 1–11.

https://doi.org/10.1016/J.PHARMTHERA.2018.02.013.
(44) Escrevente, C.; Keller, S.; Altevogt, P.; Costa, J. Interaction and Uptake of Exosomes by Ovarian Cancer Cells. *BMC Cancer* **2011**, *11* (1), 108. https://doi.org/10.1186/1471-2407-11-108.
(45) Christianson, H. C.; Svensson, K. J.; van Kuppevelt, T. H.; Li, J. P.; Belting, M. Cancer Cell Exosomes Depend on Cell-Surface Heparan Sulfate Proteoglycans for Their Internalization and Functional Activity. *Proc Natl Acad Sci U S A* **2013**, *110* (43), 17380–17385. https://doi.org/10.1073/pnas.1304266110.
(46) Parolini, I.; Federici, C.; Raggi, C.; Lugini, L.; Palleschi, S.; De Milito, A.; Coscia, C.; Iessi, E.; Logozzi, M.; Molinari, A.; Colone, M.; Tatti, M.; Sargiacomo, M.; Fais, S. Microenvironmental PH Is a Key Factor for Exosome Traffic in Tumor Cells. *J Biol Chem* **2009**, *284* (49), 34211–34222. https://doi.org/10.1074/jbc.M109.041152.
(47) Svensson, K. J.; Christianson, H. C.; Wittrup, A.; Bourseau-Guilmain, E.; Lindqvist, E.; Svensson, L. M.; Morgelin, M.; Belting, M. Exosome Uptake Depends on ERK1/2-Heat Shock Protein 27 Signaling and Lipid Raft-Mediated Endocytosis Negatively Regulated by Caveolin-1. *J Biol Chem* **2013**, *288* (24), 17713–17724. https://doi.org/10.1074/jbc.M112.445403.
(48) Christianson, H. C.; Svensson, K. J.; Van Kuppevelt, T. H.; Li, J. P.; Belting, M. Cancer Cell Exosomes Depend on Cell-Surface Heparan Sulfate Proteoglycans for Their Internalization and Functional Activity. *Proc. Natl. Acad. Sci. U. S. A.* **2013**, *110* (43), 17380–17385. https://doi.org/10.1073/pnas.1304266110.
(49) Vidal, F.; Vásquez, P.; Díaz, C.; Nova, D.; Alderete, J.; Guzmán, L. Mechanism of PAMAM Dendrimers Internalization in Hippocampal Neurons. *Mol. Pharm.* **2016**, *13* (10), 3395–3403. https://doi.org/10.1021/acs.molpharmaceut.6b00381.
(50) Saovapakhiran, A.; D'Emanuele, A.; Attwood, D.; Penny, J. Surface Modification of PAMAM Dendrimers Modulates the Mechanism of Cellular Internalization. *Bioconjug. Chem.* **2009**, *20* (4), 693–701. https://doi.org/10.1021/bc8002343.
(51) Mittendorf, E. A.; Philips, A. V; Meric-Bernstam, F.; Qiao, N.; Wu, Y.; Harrington, S.; Su, X.; Wang, Y.; Gonzalez-Angulo, A. M.; Akcakanat, A.; Chawla, A.; Curran, M.; Hwu, P.; Sharma, P.; Litton, J. K.; Molldrem, J. J.; Alatrash, G. PD-L1 Expression in Triple-Negative Breast Cancer. *Cancer Immunol. Res.* **2014**, *2* (4), 361–370. https://doi.org/10.1158/2326-6066.CIR-13-0127.
(52) Zhang, J.; Zhang, G.; Zhang, W.; Bai, L.; Wang, L.; Li, T.; Yan, L.; Xu, Y.; Chen, D.; Gao, W.; Gao, C.; Chen, C.; Ren, M.; Jiao, Y.; Qin, H.; Sun, Y.; Zhi, L.; Qi, Y.; Zhao, J.; Liu, Q.; Liu, H.; Wang, Y. Loss of RBMS1 Promotes Anti-Tumor Immunity through Enabling PD-L1 Checkpoint Blockade in Triple-Negative Breast Cancer. *Cell Death Differ.* **2022**, *29* (11), 2247–2261. https://doi.org/10.1038/s41418-022-01012-0.
(53) Bertrand, N.; Grenier, P.; Mahmoudi, M.; Lima, E. M.; Appel, E. A.; Dormont, F.; Lim, J.-M.; Karnik, R.; Langer, R.; Farokhzad, O. C. Mechanistic Understanding of in Vivo Protein Corona Formation on Polymeric Nanoparticles and Impact on Pharmacokinetics. *Nat. Commun.* **2017**, *8* (1), 777. https://doi.org/10.1038/s41467-017-00600-w.
(54) Mecke, A.; Majoros, I. J.; Patri, A. K.; Baker, J. R.; Banaszak Holl, M. M.; Orr, B. G. Lipid Bilayer Disruption by Polycationic Polymers: The Roles of Size and Chemical Functional Group. *Langmuir* **2005**, *21* (23), 10348–10354. https://doi.org/10.1021/la050629l.
(55) Hong, S.; Leroueil, P. R.; Janus, E. K.; Peters, J. L.; Kober, M.-M.; Islam, M. T.; Orr, B.

G.; Baker, J. R.; Banaszak Holl, M. M. Interaction of Polycationic Polymers with Supported Lipid Bilayers and Cells: Nanoscale Hole Formation and Enhanced Membrane Permeability. *Bioconjug. Chem.* **2006**, *17* (3), 728–734. https://doi.org/10.1021/bc060077y.

(56) Albertazzi, L.; Serresi, M.; Albanese, A.; Beltram, F. Dendrimer Internalization and Intracellular Trafficking in Living Cells. *Mol. Pharm.* **2010**, *7* (3), 680–688. https://doi.org/10.1021/mp9002464.

(57) Saovapakhiran, A.; D'Emanuele, A.; Attwood, D.; Penny, J. Surface Modification of PAMAM Dendrimers Modulates the Mechanism of Cellular Internalization. *Bioconjug. Chem.* **2009**, *20* (4), 693–701. https://doi.org/10.1021/bc8002343.

(58) Hong, S.; Hessler, J. A.; Banaszak Holl, M. M.; Leroueil, P.; Mecke, A.; Orr, B. G. Physical Interactions of Nanoparticles with Biological Membranes: The Observation of Nanoscale Hole Formation. *J. Chem. Heal. Saf.* **2006**, *13* (3), 16–20. https://doi.org/10.1016/j.chs.2005.09.004.

(59) Ferguson, S. W.; Nguyen, J. Exosomes as Therapeutics: The Implications of Molecular Composition and Exosomal Heterogeneity. *J. Control. Release* **2016**, *228*, 179–190. https://doi.org/https://doi.org/10.1016/j.jconrel.2016.02.037.

(60) Horibe, S.; Tanahashi, T.; Kawauchi, S.; Murakami, Y.; Rikitake, Y. Mechanism of Recipient Cell-Dependent Differences in Exosome Uptake. *BMC Cancer* **2018**, *18*, 47. https://doi.org/10.1186/s12885-017-3958-1.

(61) Yang, J.; Zhang, Q.; Chang, H.; Cheng, Y. Surface-Engineered Dendrimers in Gene Delivery. *Chem. Rev.* **2015**, *115* (11), 5274–5300. https://doi.org/10.1021/cr500542t.

(62) Kamerkar, S.; Lebleu, V. S.; Sugimoto, H.; Yang, S.; Ruivo, C. F.; Melo, S. A.; Lee, J. J.; Kalluri, R. Exosomes Facilitate Therapeutic Targeting of Oncogenic KRAS in Pancreatic Cancer. *Nature* **2017**, *546* (7659), 498–503. https://doi.org/10.1038/nature22341.

(63) Ko, Y. T.; Bhattacharya, R.; Bickel, U. Liposome Encapsulated Polyethylenimine/ODN Polyplexes for Brain Targeting. *J Control Release* **2009**, *133* (3), 230–237. https://doi.org/10.1016/j.jconrel.2008.10.013.

(64) Laulagnier, K.; Motta, C.; Hamdi, S.; Roy, S.; Fauvelle, F.; Pageaux, J.-F.; Kobayashi, T.; Salles, J.-P.; Perret, B.; Bonnerot, C.; Record, M. Mast Cell- and Dendritic Cell-Derived Exosomes Display a Specific Lipid Composition and an Unusual Membrane Organization. *Biochem. J.* **2004**, *380* (Pt 1), 161–171. https://doi.org/10.1042/bj20031594.

(65) Jiang, X.; Bugno, J.; Hu, C.; Yang, Y.; Herold, T.; Qi, J.; Chen, P.; Gurbuxani, S.; Arnovitz, S.; Strong, J.; Ferchen, K.; Ulrich, B.; Weng, H.; Wang, Y.; Huang, H.; Li, S.; Neilly, B. M.; Larson, A. R.; Le Beau, M. M.; Bohlander, K. S.; Jin, J.; Li, Z.; Bradner, J. E.; Hong, S.; Chen, J. Eradication of Acute Myeloid Leukemia with FLT3 Ligand–Targeted miR-150 Nanoparticles. *Cancer Res.* **2016**, 76 (15), 4470-4480. https://doi.org/10.1158/0008-5472.CAN-15-2949.

(66) Nair, A.; Bu, J.; Bugno, J.; Rawding, A. P.; Kubiatowicz, J. L.; Jeong, W.J.; Hong, S. Size-Dependent Drug Loading, Gene Complexation, Cell Uptake, and Transfection of a Novel Dendron-Lipid Nanoparticle for Drug/Gene Co-delivery. *Biomacromolecules* **2021**, 22, 9, 3746-3755. https://doi.org/10.1021/acs.biomac.1c00541.

TOC Graphic